

NUMERICAL SIMULATIONS OF THE TRANSITION FROM FLEXURAL CRACKING TO SHEAR TO FLEXURAL CRUSHING FAILURES IN PRE-NOTCHED REINFORCED CONCRETE BEAMS

HONGJIE CHEN^{*}, YING YU^{*}, CHENGSHENG LI^{*},
FEDERICO ACCORNERO^{*}, ALBERTO CARPINTERI^{*}

^{*} Shantou University, Department of Civil Engineering and Smart Cities,
Daxue Road, 515063 Shantou, China
e-mail: 21hjchen1@stu.edu.cn, www.stu.edu.cn

Key words: Crack propagation, Minimum reinforcement, Ductile-to-brittle transition, Size-scale effects

Abstract: This study predicts the transition between flexural cracking, shear, and flexural crushing failure modes in reinforced concrete (RC) beams through a series of four-point bending simulations on 48 pre-notched specimens. The upcoming experimental setup explores the influence of key parameters, including: (1) longitudinal reinforcement ratios ranging from 0.13% to 2.26%; (2) slenderness ratios (λ) from 3 to 24; (3) beams of varying size-scale with a constant reinforcement ratio; (4) beams of varying size-scale with a constant reinforcement area. The bridged crack model is applied to assess crack propagation and failure mechanisms, providing insight into the mechanical response, ultimate load capacity, and the critical cracks leading to failure. Dimensionless numbers N_P and N_C are used to capture the brittleness transitions between different failure modes, offering a unified theoretical framework for evaluating these behaviors. The results provide valuable data for understanding the scale effects on brittleness in RC beams.

1 INTRODUCTION

The determination of the shear strength of reinforced concrete (RC) beam elements without transverse reinforcement has been deeply investigated in literature since the beginnings of the development of RC technology. Another remarkable line of studies is due to Carpinteri and co-workers who proposed an approach to the problem based on fracture mechanics and dimensional analysis background and performed several experimental tests. They initially studied the problem of minimum reinforcement in RC beams and the related brittle or ductile bending failure mechanism [1–7]. These studies were then extended to include the effect of fibres reinforcement [8–10], shear and concrete crushing failures [11–13,15], influence of axial

force [14] and size effects, which were introduced through dimensionless brittleness numbers. Structural elements having the same brittleness number show the same mechanical behavior. The works by Carpinteri and coauthors share the common idea that failure is caused by the formation and propagation of a critical crack. This concept has been used both for the early works on bending failure and specifically in mixed bending/shear works where the shape of the critical crack was reported from experimental testing [12,15].

The aim of this work is to provide the scientific community with the numerical simulations data of a series of four-point bending on pre-notched specimens. In total 48 beams will be tested, we use numerical simulations to predict some relative data in advance. The outline of the paper is as

follows: Section 2 is devoted to the description of the experimental program, by detailing the reinforcement amount and the beam size. Section 3 shows the load carrying capacity of each beam simulated numerically. Section 4 predicts the failure form of each beam based on the dimensionless analysis. Finally, Section 5 draws conclusions.

2 EXPERIMENTAL PROGRAM

An extended experimental program was carried out in the Structures Laboratory of Shantou University to investigate the failure mechanisms and cracking modes of concrete beams reinforced only with longitudinal reinforcement. This experiment consists of four sets of beams, and the effects of these variables on concrete beams can be obtained by varying reinforcement ratio, length-to-depth ratio, and the size-scale. The experimental setup explores the influence of key parameters, including: (1) longitudinal reinforcement ratios ranging from 0.13% to 2.26%; (2) slenderness ratios (λ) from 3 to 24; (3) beams of varying size-scale with a constant reinforcement ratio; (4) beams of varying size-scale with a constant reinforcement area.

2.1 Specimen geometry and test setup

The test specimen has span S , depth h , width b , and notch depth a_0 . The reinforcement ratio ρ is equal to $A_s / (hb)$. The beams are simply supported and loaded in four-point bending (see Fig. 1).

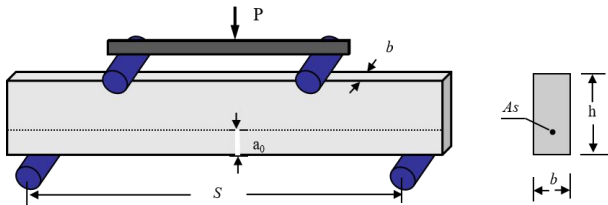


Figure 1: Test setup.

Four series of specimens will be tested, totaling 16 different types of beams. Table 1 lists the geometric parameters and longitudinal reinforcement amounts for all beams. It is worth noting that, in order to be consistent with the definitions of the brittleness numbers

N_p and N_c [2,15,16], all parameters are normalized by the beam depth h , which will be used to interpret the results in the next sections. For each beam type, three specimens were prepared, in order to have some statistics of the results.

Table 1:-Specimen series

	b (mm)	h (mm)	s (mm)	A_s
Effect of steel reinforcement (Series 1)	200	200	1200	1 Φ 8
	200	200	1200	2 Φ 8
	200	200	1200	4 Φ 8
	200	200	1200	4 Φ 12
	200	200	1200	8 Φ 12
Effect of beam Slenderness (Series 2)	200	200	600	4 Φ 12
	200	200	1200	4 Φ 12
	200	200	2400	4 Φ 12
	200	200	4800	4 Φ 12
Size effect with constant reinforcement t area (Series 3)	200	200	1200	2 Φ 12
	200	400	2400	2 Φ 12
	200	800	4800	2 Φ 12
	400	1600	9600	2 Φ 12
	200	200	1200	4 Φ 12
Size effect with constant reinf. Ratio (Series 4)	200	400	2400	3 Φ 20
	200	800	4800	6 Φ 20
	200	800	4800	6 Φ 20

2.2 Material properties and specimen preparation

Preparation of concrete, reinforcement arrangement and casting were accomplished in a concrete beam preparation plant in Shantou, Guangdong Province (see Fig. 2).

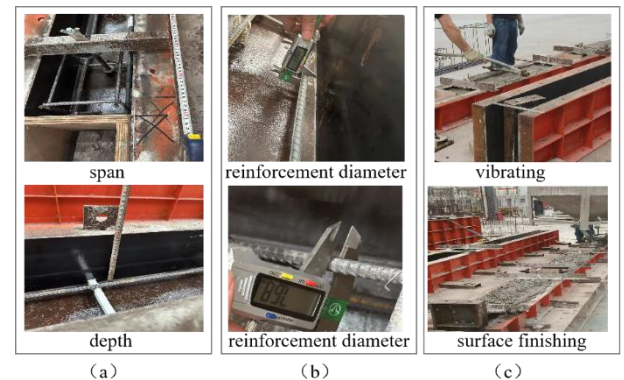


Figure 2: Specimen preparation: (a) formworks; (b) reinforcement arrangement; (c) concrete casting.

The main prescriptions for concrete are: strength class, as defined by GB/T 50107—2010 [19], equal to C30, maximum aggregate size equal to 20 mm (defined through the slump test according to JGJ 2011 [20]). The actual mechanical properties of concrete were assessed with specific tests carried out 28 days after casting. The compression strength, f_c , was measured on 150 x 150 x 150 mm cubic specimens; the secant value of the elastic modulus, E_c , was assessed on cylindrical specimens 100 mm in diameter and 300 mm in depth, following the Standards GB/T 50081-2019 [21]; the fracture energy, G_F , was evaluated by means of three-point-bending tests carried out on pre-notched beams following the procedure prescribed by RILEM Recommendation TC-89 [22].

Table 2: Mechanical properties of concrete

f_{ck} (Mpa)	f_c (Mpa)	E_c (Mpa)	G_F (N/mm)
30	21.43	32836	0.14

As regards the reinforcement bars, only three diameters have been used, 8, 12 and 20 mm, in order to limit the effect of the steel–concrete bond properties (note that 8 mm bars were used to provide the correct amount of reinforcement only in the case of very low percentages). The HRB335 steel was used, characterized by a yielding strength standard value of 335 MPa and an ultimate standard value strength of 490 MPa. The design yield strength is 300 MPa and the design ultimate value strength is 445 MPa.

Table 3: Mechanical properties of steel

Φ (mm)	f_y (Mpa)	f_t (Mpa)
8	300	455
12	300	455
20	300	455

3 SIMULATIONS BY THE COHESIVE/OVERLAPPING CRACK MODEL (COCM)

This section presents and discusses the

results of the simulations tests. The numerical simulations is based on the data obtained from the Cohesive/Overlapping Crack Model [17]. This section focuses on the load vs. deflection curves to predict the failure modes of the beams.

3.1 Effect of the reinforcement amount

The first series of specimens was designed to analyze the effect of the reinforcement amount on the load-carrying capacity and the crack pattern. It consists of 5 types of beams, having the same size and different reinforcement percentages, ρ , varying in the range 0.13% to 2.26% (see Fig. 3).

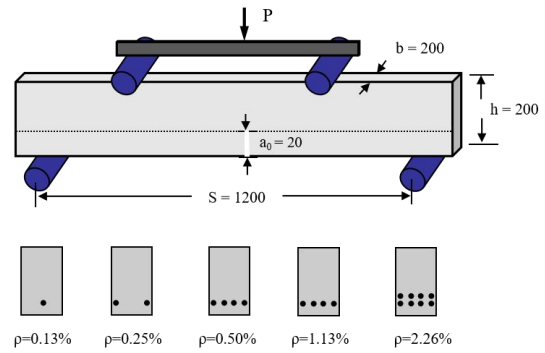


Figure 3: Set of beams used to analyze the effect of the reinforcement amount, ρ .

With numerical simulations, it is possible to obtain the load-deflection curves (Fig. 4). From the figure, the beams with reinforcement ratio 0.13% to 1.13% are ductile and the beams with reinforcement ratio 2.26% show brittle crushing failure.

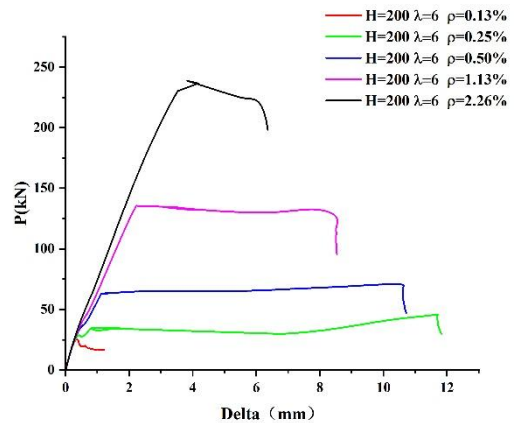


Figure 4: Load vs. mid-span deflection curves for the series of beams designed to analyze the effect of the reinforcement amount.

3.2 Slenderness effect

The slenderness effect was analyzed by considering beams with a constant reinforcement ratio $\rho = 1.13\%$, a constant depth $h = 200$ mm, and different beam spans varying from 600 to 4800 mm (Fig. 5).

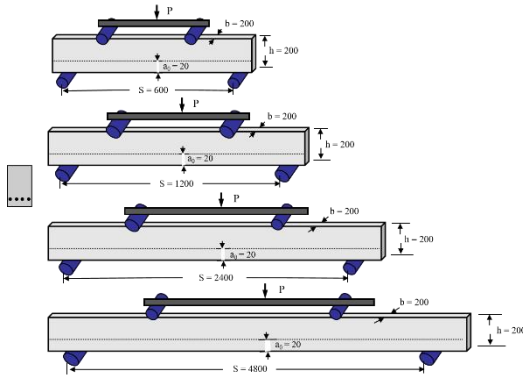


Figure 5: Set of beams used to analyze the slenderness effect with constant reinforcement ratio, $\rho = 1.13\%$.

With numerical simulations, it is possible to obtain the load-deflection curves (Fig. 6). The beams with slenderness 6 to 24 are ductile, whereas for slenderness 3 a brittle crushing is detected.

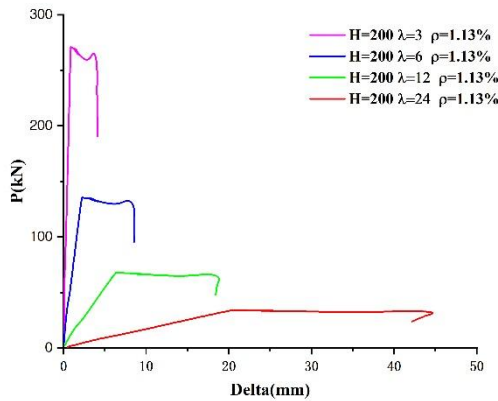


Figure 6: Load vs. mid-span deflection curves for the series of beams designed to analyze the slenderness effect with constant reinforcement ratio.

3.3 Size-scale effect

The size-scale effect is analyzed by increasing the beam depth from 200 to 1600

mm (Fig. 7). Then, a set of beams will be tested to analyze the size-scale effect with a constant reinforcement percentage, $\rho = 1.13\%$ (Fig. 9).

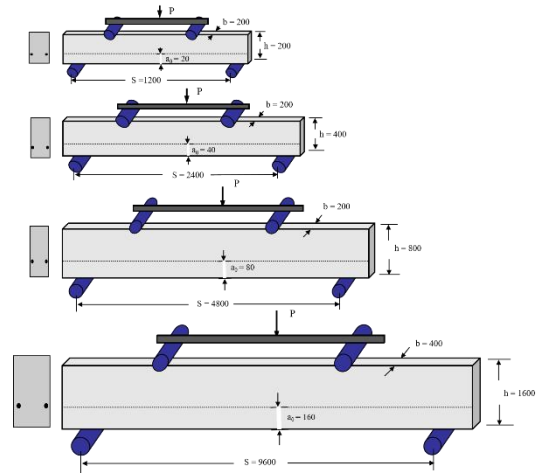


Figure 7: Set of beams with different size-scales and constant reinforcement area, $A_s = 226 \text{ mm}^2$.

With numerical simulations, it is possible to obtain the load-deflection curves (Fig. 8). The beams with constant reinforcement area are ductile except for $h=1600$ mm that is brittle.

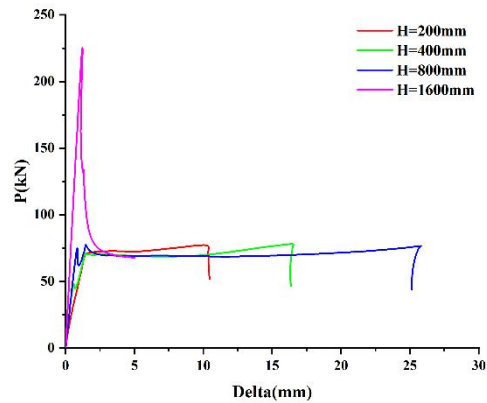


Figure 8: Load vs. mid-span deflection curves for the series of beams designed to analyze the size-scale effect with constant reinforcement area.

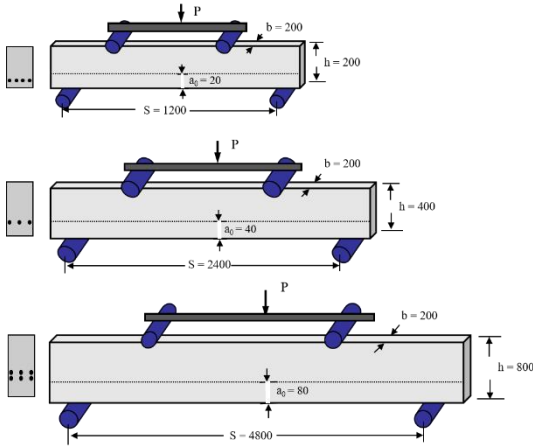


Figure 9: Set of beams used to analyze the size-scale effect with constant reinforcement percentage $\rho = 1.13\%$.

With numerical simulations, it is possible to obtain the load-deflection curves (Fig. 10). The beams with constant reinforcement percentage are ductile.

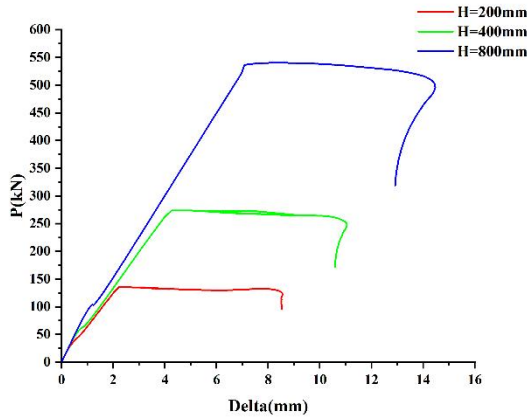


Figure 10: Load vs. mid-span deflection curves for the series of beams designed to analyze the size-scale effect with constant reinforcement percentage.

4 DIMENSIONAL ANALYSIS

Recent studies by the present authors [13,15,18] have shown that the failure mode transitions in RC beams can be conveniently analyzed on the basis of three dimensionless parameters, namely the shear slenderness, λ_s , equal to $S/(2h)$, and two brittleness numbers, N_P and N_C , obtained by applying the Buckingham's Π -theorem of dimensional analysis to the functional relationship of the geometrical and mechanical parameters involved in the problem. The procedure yields

to reduce the number of dimensionless variables [2,15,23]:

$$N_P = \rho \frac{f_y h^{0.5}}{K_{IC}} \quad (1)$$

introduced by Carpinteri since 1981 [1], and

$$N_C = \rho \frac{f_C h^{0.5}}{K_{IC}} \quad (2)$$

introduced by Carpinteri et al [16,17]. The dimensional analysis procedure applied to derive N_P and N_C provides the expression for the dimensionless load:

$$\tilde{P} = \frac{P}{K_{IC} h^{0.5} W} \quad (3)$$

In Eqs. (1) to (3), K_{IC} is the concrete fracture toughness, which has been herein computed by means of the fundamental Irwin's relation, holding in the framework of linear elastic fracture mechanics:

$$K_{IC} = \sqrt{E_c G_F} \quad (4)$$

N_P includes the effects of the reinforcement amount and strength, the concrete toughness, and the structural size-scale, whereas N_C introduces the effect of the concrete compression strength. In dimensionless terms, the structural response is expected to be only a function of the three dimensionless numbers. In particular, physical similarity is predicted when the three dimensionless parameters are constant, although the single mechanical and geometrical properties vary [15,23,24]. The values of the three dimensionless numbers are reported in Table 4 for all the beam types. It is worth noting that, in the first three series of beams, both N_P and N_C vary.

Table 4: Dimensionless numbers for each type of beam.

	N_P	N_C	P_{COCM} (kN)	\tilde{P}
Effect of steel	0.09	5.00	28	0.15
reinforcement	0.17	5.00	45	0.23
ratio	0.35	5.00	70	0.36
(Series 1)	0.79	5.00	130	0.68
	1.58	5.00	240	1.25

Effect of beam	0.79	5.00	270	1.41
Slenderness (Series 2)	0.79	5.00	135	0.70
	0.79	5.00	78	0.41
	0.79	5.00	34	0.18
Size-scale effect with constant reinforcement area(Series 3)	0.39	5.00	78	0.41
	0.28	7.07	78	0.29
	0.20	9.99	78	0.20
	0.08	14.13	230	0.21
Size-scale effect with constant reinforcement ratio(Series 4)	0.79	5.00	137	0.71
	1.11	7.07	270	0.99
	1.58	9.99	570	1.48

5 CONCLUSIONS

This paper makes a multifaceted contribution to the study of the shear strength of RC members without transverse reinforcement. According to the Global Failure Mode Transition Scheme [25], a double transition from flexural to shear failure and from shear to crushing failure is obtained: by increasing the reinforcement area, by decreasing the scale with constant reinforcement area, by increasing the scale with constant reinforcement percentage, and by decreasing the beam slenderness. We use numerical simulations to predict in advance the relevant data for the beams to be tested, providing a more convenient solution for the experiments.

Moreover, we are about to carry out the experimental program presented in this paper, which is unique in the recent literature in terms of the number of specimens tested and the type of parameters studied, and the results will be able to constitute a comprehensive database that will be very useful for future research work.

REFERENCES

- [1] Carpinteri A. A fracture mechanics model for reinforced concrete collapse. *IABSE colloquium on advanced mechanics of reinforced concrete*, Delft, The Netherlands. 1981. pp.17 - 30.
- [2] Carpinteri A., 1984. Stability of fracturing process in RC beams. *J Struct Eng.*

110:544 - 58.

- [3] Bosco C, Carpinteri A, Debernardi PG., 1990. Fracture of reinforced concrete: Scale effect and snap-back instability. *Eng Fract Mech.* **35(4 - 5):228 - 36.**
- [4] Bosco C, Carpinteri A, Debernardi PG., 1990. Minimum reinforcement in high-strength concrete. *J Struct Eng.* **116(2):228 - 36.**
- [5] Carpinteri A., 1984. Stability of fracturing process in Rc beams. *J Struct Eng.* **110:544-58.**
- [6] Carpinteri A, Ed. Minimum reinforcement in concrete members. London: Number 24 in ESIS Publications. *Elsevier*; 1999.
- [7] Corrado M, Cadamuro E, Carpinteri A., 2011. Dimensional analysis approach to study snap back-to-softening-to-ductile transitions in lightly reinforced quasi-brittle materials. *Int J Fract.* **172(1):53 - 63.**
- [8] Carpinteri A, Massabò R., 1997. Continuous vs. discontinuous bridged-crack model for fiber reinforced materials in flexure. *Int J Solids Struct.* **34(21):2321 - 38.**
- [9] Carpinteri A, Ferro G, Ventura G., 2003. Size effects on flexural response of reinforced concrete elements with a nonlinear matrix. *Eng Fract Mech.* **70:995-1013.**
- [10] Carpinteri A, Cadamuro E, Ventura G., 2015. Fiber-reinforced concrete in flexure: A cohesive/overlapping crack model application. *Mater Struct.* **48(1 - 2):235 - 47.**
- [11] Carpinteri A, Carmona JR, Ventura G., 2007. Propagation of flexural and shear cracks through reinforced concrete beams by the bridged crack model. *Mag Concr*

Res. **59(10)**:743 – 56.

- [12] Carpinteri A, Carmona JR, Ventura G. , 2011. Failure mode transitions in reinforced concrete beams – Part 2: Experimental tests. *ACI Struct J.* **108(3)**:286 – 93.
- [13] Carpinteri A, Corrado M, Mancini G, Paggi M. , 2009. Size-scale effects on plastic rotational capacity of reinforced concrete beams. *ACI Struct J.* **106(6)**:887 – 96.
- [14] Carpinteri A, Corrado M, Goso G, Paggi M, 2012. Size-scale effects on interaction diagrams for reinforced concrete columns. *Constr Build Mater.* **27(1)**:271 – 9
- [15] Carpinteri A, Carmona JR, Ventura G, 2011. Failure mode transitions in reinforced concrete beams-Part 1: Theoretical model. *ACI Struct J.* **108(3)**:277 – 85.
- [16] Carpinteri A, Corrado M, 2011. Upper and lower bounds for structural design of RC members with ductile response. *Eng Struct.* **33**:3432 – 41.
- [17] Accornero F, Cafarelli R, Carpinteri A, 2021. The cohesive/overlapping crack model for plain and RC beams: Scale effects on cracking and crushing failures. *Magazine of Concrete Research.* **74(9)**:433-450.
- [18] Carpinteri A, Corrado M, Ventura G. Failure mode scaling transitions in RC beams in flexure: Tensile, shearing, crushing. In: *Proceedings of the 8th international FraMCoS conference*, Toledo, Spain. 2013, pp. 31–43.
- [19] Standardization Administration of the People's Republic of China. GB/T50107-2010 *Standard for evaluation of concrete compressive strength*; 2010.
- [20] Standardization Administration of the People's Republic of China. JGJ 2011 *Specification for mix proportion design of ordinary concrete*; 2011.
- [21] Standardization Administration of the People's Republic of China. GB-T 50081-2019 *Standard for test methods of concrete physical and mechanical properties*; 2019.
- [22] RILEM TCS, 1985. Determination of the fracture energy of mortar and concrete by means of three-point bend tests on notched beams. *Mater Struct.* **18**:285–90.
- [23] Carpinteri A, Corrado M, 2010. Dimensional analysis approach to the plastic rotation capacity of over-reinforced concrete beams. *Eng Fract Mech*; **77**:1091–100.
- [24] Carpinteri A, Corrado M, 2011. Upper and lower bounds for structural design of RC members with ductile response. *Eng Struct.* **33**:3432–41.
- [25] Carpinteri A, Puzzi S, 2008. Self-similarity in concrete fracture: Size-scale effects and transition between different collapse mechanisms. *International Journal of Fracture.* **154**:167-175.